Nucleon Resonances with Hidden Charm in Coupled-Channel Models

Jia-Jun Wu[1,2], T.-S. H. Lee[2] and B. S. Zou[1,3]

[1] Institute of High Energy Physics, CAS, P.O.Box 918(4), Beijing 100049, China

[2] Physics Division, Argonne National Laboratory, Argonne, Illinois 60439, USA

[3] Theoretical Physics Center for Science Facilities, CAS, Beijing 100049, China

(Dated: Feb. 4, 2012)

arXiv:1202.1036v1 [nucl-th] 6 Feb 2012

Abstract

The model dependence of the predictions of nucleon resonances with hidden charm is investigated. We consider several coupled-channel models which are derived from relativistic quantum field theory by using (1) a unitary transformation method, and (2) the three-dimensional reductions of Bethe-Salpeter Equation. With the same vector meson exchange mechanism, we find that all models give very narrow molecular-like nucleon resonances with hidden charm in the mass range of 4.3 GeV $< M_R <$ 4.5 GeV, in consistent with the previous predictions.

I. INTRODUCTION

In the classical quark models, each baryon is made of three constituent quarks [1]. The pattern of the spectra and the static properties of the ground and low-lying excited states of baryons can be described reasonably well within these models. However, there are large deviations between the predictions from these models and the experimental data [2], such as the strong coupling of $N^*(1535)$ to the strangeness, and the mass order between $N^*(1535)$ and $\Lambda^*(1405)$. In the classical 3-quark models, the $N^*(1535)$ with (uud)-quarks is expected to be lighter than $\Lambda^*(1405)$ with (uds)-quarks. This problem may be solved by the penta-quark picture for these excited baryons. In the penta-quark models, the $N^*(1535)$ with $[uu][ds]\bar{s}$ is naturally heavier than the $\Lambda^*(1405)$ with $[ud][sq]\bar{q}$ [3]. Actually, the conventional orbital excitation energy of a original constituent quark in a baryon is already comparable to drag out a $q\bar{q}$ pair from the gluon field. As a result, some excited baryons are proposed to be meson-baryon dynamically generated states [4–10] or states with large $(qqqq\bar{q})$ components [3, 11, 12]. But because of the same resonances predicted by different models are in the similar energy region, there are always some adjustable ingredients in each model to fit the experimental data. Thus it is difficult to pin down the nature of these baryon resonances. One way to avoid such difficulty is to replace light flavor $q\bar{q}$ in these baryons by $c\bar{c}$. Brodsky *et al.* [13] proposed in the early 1980s that there are about 1% $uudc\bar{c}$ components in the proton. Recently, Refs.[14–16] have used different methods to predict some narrow hidden charm $N^*_{c\bar{c}}$ and $\Lambda^*_{c\bar{c}}$ resonances with masses above 4 GeV and widths smaller than 100 MeV. These resonances, if observed, absolutely cannot be ascribed to the conventional 3-quark states. Therefore, it is important to investigate the extent to which the predicted $N^*_{c\bar{c}}$ and $\Lambda^*_{c\bar{c}}$ resonances can be further firmly established.

In this work we focus on the predictions [14] from a Beijing-Valencia collaboration. Their results are from solving the following algebraic coupled-channel equations

$$T_{\alpha,\beta}(s) = \sum_{\gamma} V_{\alpha,\gamma}(s)\hat{G}_{\gamma}(s)T_{\gamma,\beta}(s) + V_{\alpha,\beta}(s) \tag{1}$$

where $\alpha, \beta, \gamma = \bar{D}\Sigma_c, \bar{D}\Lambda_c, \eta_c N$, and s is the square of the C.M. energy. In Eq.(1) the meson-baryon potential is based on the vector meson-exchange mechanisms of Ref.[5] and

is written in the following separable form

$$
\begin{aligned}
V_{\alpha,\alpha}(s) &= \frac{C_{\alpha,\alpha}}{4f^2}(2E_{M_\alpha}), \\
V_{\alpha,\beta}(s) &= -C_{\alpha,\beta}\frac{m_\rho^2}{4f^2}\frac{E_{M_\alpha}+E_{M_\beta}}{m_{M_\alpha}^2+m_{M_\beta}^2-2E_{M_\alpha}E_{M_\beta}-m_V^2} \qquad (\alpha\neq\beta) \qquad (2)
\end{aligned}
$$

where the E_{M_α} is the on-shell energy of the α channel's meson, and m_V is the mass of exchange vector. The factorized propagator $\hat{G}_\gamma(E)$ is calculated from either using the dimensional regularization or introducing a cutoff parameter Λ

$$
\begin{aligned}
\hat{G}(E)\to G_{DR}(E) &= \frac{2m_B}{16\pi^2}\Big\{a_\mu+\ln\frac{m_B^2}{\mu^2}+\frac{m_M^2-m_B^2+s}{2s}\ln\frac{m_M^2}{m_B^2} \\
&+ \frac{\bar{q}}{\sqrt{s}}\big[\ln(s-(m_B^2-m_M^2)+2\bar{q}\sqrt{s})+\ln(s+(m_B^2-m_P^2)+2\bar{q}\sqrt{s}) \\
&- \ln(-s-(m_B^2-m_M^2)+2\bar{q}\sqrt{s})-\ln(-s+(m_B^2-m_M^2)+2\bar{q}\sqrt{s})\big]\Big\} \qquad (3) \\
\hat{G}(E)\to G_C(E) &= \int_0^\Lambda \frac{q^2dq}{4\pi^2}\frac{2m_B(\omega_M+\omega_B)}{\omega_M\,\omega_B\,(s-(\omega_M+\omega_B)^2+i\epsilon)} \qquad (4)
\end{aligned}
$$

where $\bar{q}$ is on shell three momentum of MB system, $\omega_M=\sqrt{q^2+m_M^2}$ and $\omega_B=\sqrt{q^2+m_B^2}$. It was found that the solutions of the above equations yield few narrow resonances above 4.0 GeV.

As discussed in Ref.[14], Eqs.(1)-(4) are derived from making approximations on the Bethe-Salpeter (BS) equation. Schematically, the BS equation is (omitting the channel indices)

$$
\begin{aligned}
T(q',q,P) &= V(q',q,P) \\
&+\int d^4k V(q',k,P)\frac{1}{((\frac{P}{2}+k)^2-m_M^2+i\epsilon)((\frac{P}{2}-k)^2-m_B^2)+i\epsilon}T(k,q;P) \qquad (5)
\end{aligned}
$$

where P is the total four momentum of the system, q,q' and k are the relative momenta. For the considered vector meson-exchange, the interaction kernel is

$$
V(q,k,P) = C\frac{1}{(q-k)^2-m_V^2} \qquad (6)
$$

where C is a coupling constant. The complications in solving Eq.(5) is well known, as discussed in, for example, Ref.[17] for πN scattering. Thus approximations, such as those used [14] in obtaining Eqs.(1)-(4), are needed for practical calculations. There exist other approximations to solve BS equations and alternative approaches to derive practical hadron reaction models from relativistic quantum field theory. It is thus necessary to investigate the

extent to which the results from Ref.[14] depend on the approximations employed. This is the objective of this work. We will consider several coupled-channel models derived from using a unitary transformation method [18] and the three-dimensional reductions [19] of Bethe-Salpeter equation. These formulations have been used in studying πN scattering [18, 20, 21], NN scattering [22], and coupled-channel πN and γN reactions in the nucleon resonance region [23, 24].

In section II, we present the considered coupled-channel formulations and discuss their differences with Eqs.(1)-(4). The numerical procedures for solving the considered coupled-channel equations are described in section III. We then investigate in section IV, the numerical consequences of the differences between different coupled-channel models in predicting the resonance positions and the reaction cross sections. A summary is given in section V.

II. FORMALISM

Following Ref.[14], we assume that the interactions between the considered meson-baryon (MB) channels are due to the vector meson-exchange mechanism and can be calculated from the following interaction Lagrangian

$$\mathcal{L}_{int} = \mathcal{L}_{VVV} + \mathcal{L}_{PPV} + \mathcal{L}_{BBV} \tag{7}$$

with

$$\begin{aligned}
\mathcal{L}_{VVV} &= ig\langle V^\mu [V^\nu, \partial_\mu V_\nu]\rangle \\
\mathcal{L}_{PPV} &= -ig\langle V^\mu [P, \partial_\mu P]\rangle \\
\mathcal{L}_{BBV} &= g(\langle \bar{B}\gamma_\mu [V^\mu, B]\rangle + \langle \bar{B}\gamma_\mu B\rangle\langle V^\mu\rangle)
\end{aligned} \tag{8}$$

where P and V stand for the Pseudoscalar and Vector mesons of the 16-plet of SU(4), respectively, and B stands for the baryon. The coupling constant $g = M_V/2f$ is taken from the hidden gauge model with $f = 93$ MeV being the pion decay constant and $M_V = 770$ MeV the mass of the light vector meson.

By using Eq.(7), the invariant amplitude of the $PB \to PB$ and $VB \to VB$ transitions due to the one-vector-meson-exchange interaction, as illustrated as illustrated in Fig.1, can

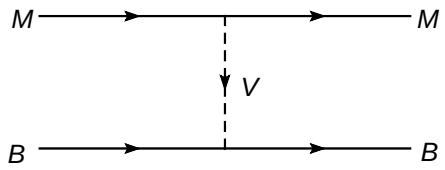


FIG. 1: One vector exchange mechanism of meson-baryon interactions.

be written as (suppressing the spin quantum numbers)

$$\mathcal{M}^{PB,I,V}(q_i,q_j) \;=\; C_{i,j}^{PB,I,V}\frac{M_V^2}{4f^2}\frac{p_V^\mu p_V^\nu/m_V^2-g^{\mu\nu}}{p_V^2-m_V^2}\bar{u}_{B_i}\gamma_\mu(p_{M_i}+p_{M_j})_\nu u_{B_j}, \tag{9}$$

$$\mathcal{M}^{VB,I,V}(q_i,q_j) \;=\; C_{i,j}^{VB,I,V}\frac{M_V^2}{4f^2}\frac{p_V^\mu p_V^\nu/m_V^2-g^{\mu\nu}}{p_V^2-m_V^2}\bar{u}_{B_i}\gamma_\mu(p_{M_i}+p_{M_j})_\nu u_{B_j}(-\varepsilon^*_{M_i}\cdot\varepsilon_{M_j}), \tag{10}$$

where the sub-indices i,j stand for the M_iB_i and M_jB_j channels, I is the total isospin of the system, V denotes the exchanged vector meson, q_i is the relative momentum of the M_iB_i channel in the center of mass frame, p_α is the the four- momentum of particle α, u_{B_i} is the Dirac spinor of the baryon B_i, and ε_{M_i} is the polarization vector of the external vector meson M_i. The coefficients $C_{i,j}^{PB,I,V}$ and $C_{i,j}^{VB,I,V}$ in Eqs.(9) and (10) are taken from Ref.[14] and listed in the Tables I and II.

TABLE I: Coefficients $C^{PB,I,V}_{M_iB_iM_jB_j}$ in the Eq.(9) for the PB system in the sector $I=1/2,3/2$, $S=0$. The exchanged vector mesons $V=\rho,\omega,D^*$ are indicated next to the values of the coefficients.

I=3/2	$\bar{D}\Sigma_c$
$\bar{D}\Sigma_c$	ρ+ω

I=1 /2	$\bar{D}\Sigma_c$	$\bar{D}\Lambda_c^+$	η_cN
$\bar{D}\Sigma_c$	-2ρ+ω	0	$-\sqrt{3/2}D^*$
$\bar{D}\Lambda_c^+$	0	ω	$\sqrt{3/2}D^*$
η_cN	$-\sqrt{3/2}D^*$	$\sqrt{3/2}D^*$	0

TABLE II: Coefficients $C^{VB,I,V}_{M_iB_i\to M_jB_j}$ in the Eq.(10) for the VB system in the sector $I=1/2,3/2$, $S=0$. The exchanged vector mesons $V=\rho,\omega,D^*$ are indicated next to the values of the coefficients.

I=3/2	$\bar{D}^*\Sigma_c$
$\bar{D}^*\Sigma_c$	ρ+ω

I=1 /2	$\bar{D}^*\Sigma_c$	$\bar{D}^*\Lambda_c^+$	$J/\psi N$	ρN
$\bar{D}^*\Sigma_c$	-2ρ+ω	0	$-\sqrt{3/2}D^*$	$-1/2D^*$
$\bar{D}^*\Lambda_c^+$	0	ω	$\sqrt{3/2}D^*$	$-3/2D^*$
$J/\psi N$	$-\sqrt{3/2}D^*$	$\sqrt{3/2}D^*$	0	0
ρN	$-1/2D^*$	$-3/2D^*$	0	-2ρ

We consider the coupled-channel models derived by using the unitary transformation method of Ref.[10, 18] and the three-dimensional reductions of Bethe-Salpeter equations employed in Ref.[21]. In the center of mass (CM) frame, the scattering equations within these models can be cast into the following general form (suppressing the spin quantum numbers)

$$\begin{aligned}\hat{T}^{\alpha,I}(\vec{q}_i,\vec{q}_j,\sqrt{s}) &= \hat{V}^{\alpha,I}(\vec{q}_i,\vec{q}_j,\sqrt{s}) \\ &+\sum_k\int d\vec{q}_k\hat{V}^{\alpha,I}(\vec{q}_i,\vec{q}_k,\sqrt{s})\frac{N(\vec{q}_k,\sqrt{s})}{\sqrt{s}-E_{M_k}(\vec{q}_k)-E_{B_k}(\vec{q}_k)+i\epsilon}\hat{T}^{\alpha,I}(\vec{q}_k,\vec{q}_j,\sqrt{s})\end{aligned} \tag{11}$$

where $\alpha=PB,VB$, $\vec{q}_i$ is the relative three-momentum in channel i, $\sqrt{s}$ is the total energy, and $E_{\alpha_i}(\vec{q}_i)=\sqrt{m^2_{\alpha_i}+\vec{q}_i^{\,2}}$ is the energy of the particle $\alpha=M,B$ with a mass m_{α_i}. All external particles in the MB channels are on their mass-shell. Explicitly, we choose

$$\begin{aligned}\vec{q}_i &= \vec{p}_{M_i}=-\vec{p}_{B_i}\,, \\ p_{M_i} &= (E_{M_i}(\vec{p}_{M_i}),\vec{p}_{M_i})\,, \\ p_{B_i} &= (E_{B_i}(\vec{p}_{B_i}),\vec{p}_{B_i})\end{aligned} \tag{12}$$

In Eq.(11), the calculation of the driving term $\hat{V}^{\alpha,I}(\vec{q}_i,\vec{q}_j,\sqrt{s})$ from the invariant amplitude $\mathcal{M}^{\alpha,I,V}(q_i,q_j)$ of Eqs.(9)-Eq.(10) and the function $N(\vec{q}_k,\sqrt{s})$ in the propagator depend

on the approximations used in deriving the above three-dimensional equations from the relativistic quantum field theory. In the following, we specify these two ingredients in each model.

A. Model based on unitary transformation method

1. $N(\vec{q}_k, \sqrt{s}) = 1$

2. The driving term is calculated from the invariant amplitudes $\mathcal{M}$ of Eqs.(9)-(10) by expressing the four-momentum of the exchanged vector meson in terms of the incloming and outgoing momenta. Explicitly, we use Eq.(9) for $PB \to PB$ to get

$$\begin{aligned}
&\hat{V}^{PB,I,V}(\vec{q}_i, \vec{q}_j) \\
&= C_{i,j}^{PB,I,V} \frac{M_V^2}{4f^2} \bar{u}_{B_j} [\gamma_\mu (p_{M_i} + p_{M_j})_\nu] u_{B_i} \\
&\times \frac{1}{2} \left(\frac{\frac{(p_{M_i} - p_{M_j})^\mu (p_{M_i} - p_{M_j})^\nu}{m_V^2} - g^{\mu\nu}}{(p_{M_i} - p_{M_j})^2 - m_V^2} + \frac{\frac{(p_{B_j} - p_{B_i})^\mu (p_{B_j} - p_{B_i})^\nu}{m_V^2} - g^{\mu\nu}}{(p_{B_j} - p_{B_i})^2 - m_V^2} \right),
\end{aligned} \tag{13}$$

   where the kinematic variables are given in Eq.(12).

   The procedure for calculating the $VB \to VB$ from Eq.(10) is same since the factor $-\epsilon_{M_i}^* \cdot \epsilon_{M_j}$ does not depend on p_V of the exchanged vector meson.

B. Models based on three-dimensional reductions

We consider the three-dimensional reductions developed by Kadyshevsky, Blankenbecler and Sugar, and Thompson,as explained in Ref.[21]. All have the same form of the potential which is defined by setting the time component of the four-momentum of the exchanged vector meson V to zero. By using Eq.(9) for $PB \to PB$, we get

$$\begin{aligned}
&\hat{V}^{PB,I,V}(q_i, q_j) \\
&= C_{i,j}^{PB,I,V} \frac{M_V^2}{4f^2} \frac{\bar{u}_{B_j} [\frac{(\vec{p}_V \cdot \vec{\gamma})(\vec{p}_V \cdot (\vec{p}_{M_i} + \vec{p}_{M_j}))}{M_V^2} - (E_{M_i}(\vec{p}_{M_i}) + E_{M_2}(\vec{p}_{M_j}))\gamma^0 - (\vec{p}_{M_i} + \vec{p}_{M_j}) \cdot \vec{\gamma}] u_{B_i}}{-\vec{p}_V^2 - m_V^2}
\end{aligned} \tag{14}$$

The procedure for calculating the $VB \to VB$ from Eq.(10) is same since the factor $-\epsilon_{M_i}^* \cdot \epsilon_{M_j}$ doe not depend on p_V of the exchanged vector meson.

The function $N(\vec{k}, \sqrt{s})$ of the propagator of Eq.(11) for each reduction is

1. Kadyshevsky:

$$N(q_i, \sqrt{s}) = 1 \tag{15}$$

2. Blankenbecler-Sugar :

$$N(q_i, \sqrt{s}) = \frac{2(E_{M_i}(q_i) + E_{B_i}(q_i))}{\sqrt{s} + (E_{M_i}(q_i) + E_{B_i}(q_i))} \tag{16}$$

3. Thompson:

$$N(q_i, \sqrt{s}) = \frac{(E_{M_i}(q_i) + E_{B_i}(q_i))}{\sqrt{s}} \tag{17}$$

Note that for the on-shell momentum, defined by $\sqrt{s} = E_{M_i}(q_{0i}) + E_{B_i}(q_{0i})$, $N(q_{0i}, \sqrt{s}) = 1$. Thus all models satisfy the same unitarity condition defined by the cuts of the propagators of Eq.(11).

III. CALCULATION PROCEDURES

In this section, we describe our procedures for solving the coupled-channel equations to obtain the $MB \to MB$ cross sections.

It is convenient to cast Eq.(11) into the following familiar form

$$\begin{aligned} T^{\alpha,I}(\vec{q}_i, \vec{q}_j, \sqrt{s}) \;&=\; V^{\alpha,I}(\vec{q}_i, \vec{q}_j, \sqrt{s}) \\ &+ \sum_k \int d\vec{q}_k V^{\alpha,I}(\vec{q}_i, \vec{q}_k, \sqrt{s}) \frac{1}{\sqrt{s} - E_{M_i}(\vec{q}_k) - E_{B_i}(\vec{q}_k) + i\epsilon} T^{\alpha,I}(\vec{q}_k, \vec{q}_j, \sqrt{s}) \end{aligned} \tag{18}$$

where $\alpha = PB, VB$, and

$$V^{\alpha,I}(\vec{q}_i, \vec{q}_j, \sqrt{s}) \;=\; N^{1/2}(q_i, \sqrt{s}) \sum_V \hat{V}^{\alpha,I,V}((\vec{q}_i, \vec{q}_j, \sqrt{s}) N^{1/2}(q_j, \sqrt{s}) \tag{19}$$

$$T^{\alpha,I}(\vec{q}_i, \vec{q}_j, \sqrt{s}) \;=\; N^{1/2}(q_i, \sqrt{s}) \hat{T}^{\alpha,I}((\vec{q}_i, \vec{q}_j, \sqrt{s}) N^{1/2}(q_j, \sqrt{s}) \tag{20}$$

With the normalization $< \vec{p} | \vec{p}^{\,'} >= \delta(\vec{p} - \vec{p}^{\,'})$ for plane wave states, we obtain from Eq.(18) the following coupled-channel equations in each partial wave

$$\begin{aligned} T^{J,I}_{L_1,S_1,L_2,S_2}(q_1, q_2, \sqrt{s}) \;&=\; V^{J,I}_{L_1,S_1,L_2,S_2}(q_1, q_2, \sqrt{s}) \\ &+ \sum_{L_3,S_3} \int q_3^2 dq_3 V^{J,I}_{L_1,S_1,L_3,S_3}(q_1, q_3, \sqrt{s})\; G(q_3, \sqrt{s})\; T^{J,I}_{L_3,S_3,L_2,S_2}(q_3, q_2, \sqrt{s}) \end{aligned} \tag{21}$$

where J is the total angular momentum; L_i and S_i are the orbital angular momentum and total spin of the M_iB_i channel, and the propagator is

$$G(q_i,\sqrt{s}) \quad = \frac{1}{\sqrt{s}-E_{M_i}(q_i)-E_{B_i}(q_i)} \tag{22}$$

The matrix elements of the potential in Eq.(21) can be conveniently calculated from Eq.(19) by using the LSJ-helicity transformation [23]. Explicitly, we obtain

$$\begin{aligned}
&V^{J,I}_{L_1,S_1,L_2,S_2}(q_1,q_2,\sqrt{s}) \\
&= F_{L_1,L_2}(q_1,q_2)\frac{\sqrt{(2L_1+1)(2L_2+1)}}{2J+1}\frac{1}{(2\pi)^3}\sqrt{\frac{m_{B_1}m_{B_2}}{2E_M(q_1)E_B(q_1)2E_M(q_2)E_B(q_2)}} \\
&\times\sum_V G^{I,V}_{1,2}\sum_{\lambda_{M_1}\lambda_{B_1}}\sum_{\lambda_{M_2}\lambda_{B_2}} C^{J,M_{S_1}}_{L_1,S_1,0,M_{S_1}} C^{S_1,M_{S_1}}_{j_{M_1}\lambda_{M_1},j_{B_1}-\lambda_{B_1}} C^{J,M_{S_2}}_{L_2,S_2,0,M_{S_2}} C^{S_2,M_{S_2}}_{j_{M_2}\lambda_{M_2},j_{B_2}-\lambda_{B_2}} \\
&\times N^{1/2}(q_1;\sqrt{s})<q_1;-\lambda_{B_1},\lambda_{M_1}|\mathcal{V}^J|\lambda_{M_2},-\lambda_{B_2};q_2>N^{1/2}(q_2,\sqrt{s})
\end{aligned} \tag{23}$$

where λ_α is the helicity of particle α, and by writting Eq.(13) or Eq. (14) (and also the similar forms for VB) in helicity representation we can evaluate

$$\begin{aligned}
&<q_1;-\lambda_{B_1},\lambda_{M_1}|\mathcal{V}^J|\lambda_{M_2},-\lambda_{B_2};q_2> \\
&\quad=(2\pi)\int_{-1}^{1} dcos\theta\ d^J_{\lambda_{M_1}-\lambda_{B_1},\lambda_{M_2}-\lambda_{B_2}}(\theta)\hat{V}^{PB/VB,I,V}_{\lambda_{M_1}\lambda_{B_1},\lambda_{M_2}\lambda_{B_2}}(q_1,q_2,\theta,\sqrt{s})
\end{aligned} \tag{24}$$

where $cos\theta=\hat{q}_1\cdot\hat{q}_2$, and the matrix element in the integrand can be calculated by writing Eq.(13) or Eq. (14) (and also the similar forms for VB) in helicity representation for each of the considered coupled-channel models.

In Eq.(23) $C^{J,M}_{j_1,m_{j_1},j_2,m_{j_2}}=<J,M|j_1,j_2,m_{j_1},m_{j_2}>$ is the Clebsh-Gordon coefficient, the isospin factor is

$$G^{I,V}_{1,2}=\sum_{m_{I_{M_1}}m_{I_{B_1}}}\sum_{m_{I_{M_2}}m_{I_{B_2}}} C^{I,M_I}_{I_{M_1},I_{B_1},m_{I_{M_1}},m_{I_{B_1}}} C^{I,M_I}_{I_{M_2},I_{B_2},m_{I_{M_2}},m_{I_{B_2}}}\,, \tag{25}$$

where $(I_Mm_{I_M},I_Bm_{I_B})$ are the isospin quantum numbers of MB, and the form factor is chosen as

$$F_{L_1,L_2}(q_1,q_2)=(\frac{\Lambda_V^2}{\Lambda_V^2+q_1^2})^{(\frac{L_1}{2}+2)}(\frac{\Lambda_V^2}{\Lambda_V^2+q_2^2})^{(\frac{L_2}{2}+2)}, \tag{26}$$

where the cut-off parameter Λ_V is assumed the same value for all exchanged vector mesons for simplicity.

The differential cross sections are calculated from the partial-wave amplitudes by

$$\frac{d\sigma}{d\Omega} = \frac{16\pi^4}{s}\frac{q_2}{q_1}\frac{E_{M_1}E_{B_1}E_{M_2}E_{B_2}}{(2j_{M_1}+1)(2j_{B_1}+1)}\sum_{m_{j_{M_1}}m_{j_{B_1}}}\sum_{m_{j_{M_2}}m_{j_{B_2}}}|<M_2B_2|T(\sqrt{s})|M_1B_1>|^2, \quad (27)$$

with

$$\begin{aligned}
&<M_2B_2|\ T\ (\sqrt{s})|M_1B_1> \\
&\quad = <j_{M_2}m_{j_{M_2}}j_{B_2}m_{j_{B_2}}, I_{M_2}m_{I_{M_2}}I_{B_2}m_{I_{B_2}}|T(\sqrt{s})|j_{M_1}m_{j_{M_1}}j_{B_1}m_{j_{B_1}}, I_{M_1}m_{I_{M_1}}I_{B_1}m_{I_{B_1}}> \\
&\quad = \sum_{J,I}\sum_{L_1,S_1,L_2,S_2} T^{J,I}_{L_1,S_1,L_2,S_2}(q_1,q_2,\sqrt{s})Y_{L_2,M_{L_2}}(\theta,\phi)\sqrt{\frac{2L_1+1}{4\pi}} \\
&\quad \times\ C^{J,M_J}_{L_1,S_1,0,M_{S_1}}C^{S_1,M_{S_1}}_{j_{M_1},j_{B_1},m_{j_{M_1}},m_{j_{B_1}}}C^{J,M_J}_{L_2,S_2,M_{L_2},M_{S_2}}C^{S_2,M_{S_2}}_{j_{M_2},j_{B_2},m_{j_{M_2}},m_{j_{B_2}}} \\
&\quad \times\ C^{I,M_I}_{I_{M_1},I_{B_1},m_{I_{M_1}},m_{I_{B_1}}}C^{I,M_I}_{I_{M_2},I_{B_2},m_{I_{M_2}},m_{I_{B_2}}}. \qquad (28)
\end{aligned}$$

Obviously, $M_J = M_{S_1} = m_{j_{M_1}} + m_{j_{B_1}}$, $M_{S_2} = m_{j_{M_2}} + m_{j_{B_2}}$, $M_{L_2} = (m_{j_{M_1}} + m_{j_{B_1}}) - (m_{j_{M_2}} + m_{j_{B_2}})$ and $M_I = m_{I_{M_1}} + m_{I_{B_1}} = m_{I_{M_2}} + m_{I_{B_2}}$.

IV. THE RESULTS

In this section, we show the results from four models listed in Sec.II, and then discuss their differences with previous works [14–16].

A. The results of 4 models listed in Sec.II

We first consider the model based on the unitary transformation method described in subsection II.A. We determined the resonance pole positions ($M_R = M - i\frac{\Gamma}{2}$) by using the analytic continuation method of Ref.[25]. We find that the resonance positions are sensitive to the cutoff Λ, as seen in Table III. The resonances are generated only when the cutoff is larger than 800 MeV. As the cutoff Λ changes from 800 MeV to 2000 MeV, the "binding energy" ($\Delta E = M - E_{thr}$) is changed greatly from 0.002 MeV to 23.9 MeV. The corresponding changes in imaginary parts are also very large.

These resonances are very close to the threshold of $\bar{D}\Sigma_c$ in the PB sector and $\bar{D}^*\Sigma_c$ in the VB sector. They are mainly caused by the strong attractive potential from the t-channel ρ meson exchange in $\bar{D}\Sigma_c \to \bar{D}\Sigma_c$ and $\bar{D}^*\Sigma_c \to \bar{D}^*\Sigma_c$ processes. The situation here is different from the case when only light flavors are involved. For the πN interaction,

there is no resonance below the πN threshold, although the t-channel ρ meson exchange also provides attractive potential there with a similar coupling constant. The differences between two cases are mainly from the term $(p_{M_i} + p_{M_j})$ in Eq.(13). The potential is proportional to $(m_{M_i} + m_{M_j})$ near the threshold of system. For the $\bar{D}\Sigma_c$ case, $(m_{M_i} + m_{M_j}) \sim 4$ GeV, while it is about 0.3 GeV for the πN case. Hence the attractive potential of $\bar{D}\Sigma_c$ is an order of magnitude stronger than that of πN. This give a natural explanation why the PB system with heavy quarks can have quasi-bound states while the corresponding pure light quark sector cannot. The similar thing happens also for the VB system.

TABLE III: The pole position $(M - i\Gamma/2)$ and "binding energy" $(\Delta E = E_{thr} - M)$ for different cut-off parameter Λ and spin-parity J^P. The threshold E_{thr} is 4320.79 MeV of $\bar{D}\Sigma_c$ in PB system and 4462.18 MeV of $\bar{D}^*\Sigma_c$ in VB system. The unit for the listed numbers is MeV.

		PB System		VB System	
$J^p = \frac{1}{2}^-$	Λ	$M - i\Gamma/2$	ΔE	$M - i\Gamma/2$	ΔE
	650	-	-	-	-
	800	-	-	$4462.178 - 0.002i$	0.002
	1200	$4318.964 - 0.362i$	1.826	$4459.513 - 0.417i$	2.667
	1500	$4314.531 - 1.448i$	6.259	$4454.088 - 1.662i$	8.092
	2000	$4301.115 - 5.835i$	19.68	$4438.277 - 7.115i$	23.90
$J^p = \frac{3}{2}^-$					
	650	-	-	-	-
	800	-	-	$4462.178 - 0.002i$	0.002
	1200	-	-	$4459.507 - 0.420i$	2.673
	1500	-	-	$4454.057 - 1.681i$	8.123
	2000	-	-	$4438.039 - 7.268i$	23.14

The three other models based on three-dimensional reductions in subsection II.B give similar results as shown in Table IV, together with those from the model based on unitary transformation method, taking the cut-off parameter $\Lambda = 1500$ MeV. The corresponding

results for the total cross section of $\eta_c p \to \eta_c p$ are shown in Fig.2. All these four models predict a resonance below the $\bar{D}\Sigma_c$ threshold. The masses and widths of the resonances from these different models are almost the same.

TABLE IV: Comparison for 4 models with the cut-off $\Lambda = 1500$ MeV and $J^P = 1/2^-$ for PB system, where the threshold energy E_{thr} is 4320.79 MeV of $\bar{D}\Sigma_c$. "A" is for the model based on unitary transformation method; "B" is for Kadyshevsky model; "C" is for Blankenbecler-Sugar model; "D" is for Thompson model. ΔE_A and Γ_A are the binding energy and width for the case A. The unit is MeV.

Models	$M - i\Gamma/2$	ΔE	$\lvert\frac{\Delta E - \Delta E_A}{\Delta E_A}\rvert$	$\lvert\frac{\Gamma - \Gamma_A}{\Gamma_A}\rvert$
A	$4314.531 - 1.448i$	6.259	0	0
B	$4314.983 - 1.737i$	5.807	7.222%	19.96%
C	$4314.436 - 1.879i$	6.354	1.518%	29.77%
D	$4314.824 - 2.041i$	6.966	11.30%	40.95%

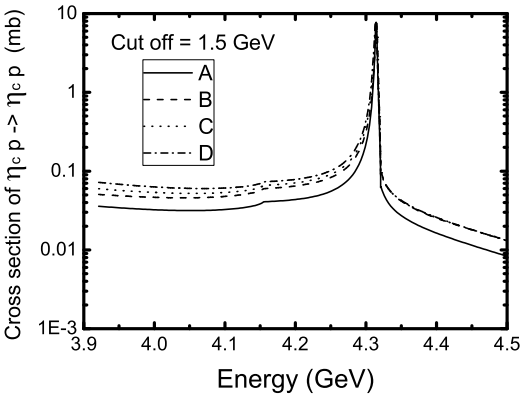


FIG. 2: The total cross section of $\eta_c p \to \eta_c p$ vs C.M. energy is shown for 4 models. The 4 lines correspond to 4 models listed in Table IV.

B. Comparison with previous works

In Ref.[14] using Valencia model, the mass and width of predicted resonance in the PB system is about 4265 MeV and 23 MeV (for $\eta_c N$ channel only). Both binding energy and width are much larger than the results in this work. All models considered in this work differ from the model used in Ref.[14] in calculating the $MB \to MB$ potentials Eqs.(9)-(10). We will get the form used in Ref.[14], if we : (1) neglect the lower component of Dirac spinor and keep only the time component γ^0; (2) set the momentum squared of the exchanged vector meson V to be $p_V^2 = (E_{M_i}^{on} - E_{M_j}^{on})^2 - (q_i^{on} - q_j^{on})^2$, where the $E_{M_i}^{on}$ and q_i^{on} are, respectively, the on-shell energy and momentum of the meson in channel i. We have investigated the effects from taking each of these two assumptions. If we only make the first simplification by neglecting spin of baryons, then the corresponding results for the resonance are shown as for potential A' in Table V; If we continue to make the second simplification by neglecting the momentum of the exchanged vector meson, the results are shown as for potential A'' of Table V. In Fig.3, we show the results corresponding to these two simplifications (dashed line for A' and dot-dashed line for A'') for the $\eta_c p \to \eta_c p$ total cross section, compared with that (solid line for A) from the model based on unitary transformation. Clearly, the second simplification shifts the resonance position to a much lower value and also increases the width significantly. This is the main reason for the difference between our present results and those from Ref.[14]. The second simplification makes p_V^2 and hence the potential V independent on the integral momentum in Eq.(5) so that Eq.(5) is simplified to Eq.(1) instead of Eq.(18) where the potential V with integral momentum dependence is inside the integration. Eq.(1) and Eq.(18) give the different results.

TABLE V: Comparison for different potential approximations with cut-off $\Lambda = 1500$ MeV and $J^P = 1/2^-$ for PB system. The threshold E_{thr} is 4320.79 MeV of $\bar{D}\Sigma_c$. "A" is for the full potential; "A'" is for the neglect of spin of baryons; "A''" is for the neglect of both spin of baryons and momentum of exchanged vector meson. ΔE_A and Γ_A are the binding energy and width for the case A. The unit is MeV.

Potential	$M - i\Gamma/2$	ΔE	$\lvert\frac{\Delta E - \Delta E_A}{\Delta E_A}\rvert$	$\lvert\frac{\Gamma - \Gamma_A}{\Gamma_A}\rvert$
A	$4314.531 - 1.448i$	6.259	0	0
A'	$4316.315 - 0.967i$	4.475	28.50%	33.22%
A''	$4229.362 - 3.914i$	91.43	1361%	170.3%

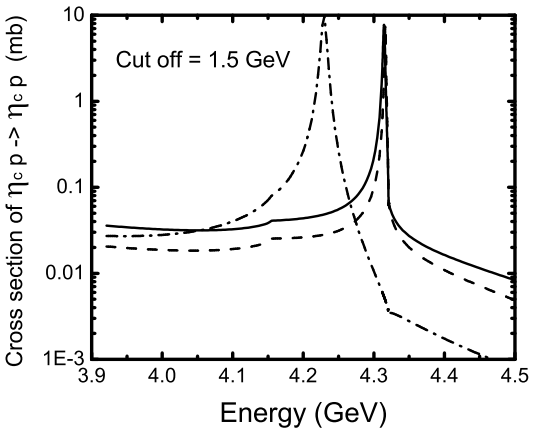


FIG. 3: The total cross section of $\eta_c p \to \eta_c p$ vs C.M. energy for different potential approximations. The solid line is for the full potential, corresponding to A in Table V; The dashed line is for the neglect of spin of baryons, corresponding to A' in Table V; The dot-dashed line is for the neglect of both spin of baryons and momentum of exchange vector, corresponding to A'' in Table V.

Besides Ref.[14], there are two later publications [15, 16] also predicting the existence of N^* around 4.3 GeV with hidden charm.

In Ref.[15], the S-wave $\Sigma_c\bar{D}$ and $\Lambda_c\bar{D}$ states with isospin I=1/2 and spin S=1/2 are dynamically investigated within the framework of a chiral constituent quark model by solving a resonating group method (RGM) equation. The calculation not only includes vector

mesons (ρ and ω) exchange, but also scalar(σ) meson exchange, which provides an additional attractive force. Therefore, the binding energy in Ref.[15] is larger than that in this work. The mass of the bound state of $\bar{D}\Sigma_c$ is about $4279 - 4316$MeV.

In Ref.[16], the Schrodinger Equation was used to find the bound state of $\bar{D}\Sigma_c$ and $\bar{D}^*\Sigma_c$ with effective meson exchange potential. For the PB system, the ρ, ω and σ exchanges were considered. They tried the different sign of coupling constants of various vertices. When they chose the ω exchange to be repulsive, and the ρ and σ exchange to be attractive, they also found the isospin 1/2 bound state of $\bar{D}\Sigma_c$ with cut off $\Lambda > 1.6$ GeV. The binding energy is about $0 - 16$MeV corresponding to $\Lambda = 1.6 - 2.2$GeV, similar to the results in this work.

V. SUMMARY

We have investigated the possible existence of nucleon resonances with hidden charm within several coupled-channel models which are derived from relativistic quantum field theory by using a unitary transformation method and the three-dimensional reductions of Bethe-Salpeter Equation. With the same vector meson exchange mechanism, we find that all models give very narrow molecular-like nucleon resonances with hidden charm in the mass range of 4.3 GeV $< M_R <$ 4.5 GeV, in consistent with the previous predictions. From our analysis, the heavy mass of particles with the c or $\bar{c}$ components would make the attractive potential stronger than the case with only light flavors. The widths of these resonances are very narrow in our models, because they need heavy vector meson D^* exchange to decay to open channels. Furthermore, we compare our results with previous works. All of models predict a resonance below the $\bar{D}\Sigma_c$ threshold. We also find that the pole position would be shift a lot if we set $p_V^2 = (E_{M_i}^{on} - E_{M_j}^{on})^2 - (q_i^{on} - q_j^{on})^2$ for the exchanged vector meson V in the potential. We look forward to find these predicted resonances with hidden charm in the reactions, such as $e\ p \ \rightarrow \ e\ J/\psi\ p$, $p\ p \ \rightarrow \ p\ \eta_c(J/\psi)\ p$, and $p\ \bar{p} \ \rightarrow \ p\ \eta_c(J/\psi)\ \bar{p}$.

Similarly the super-heavy N^* with hidden beauty should also exist although the binding energies may be not as large as given by the simple Valencia model calculation of Ref.[26].

Acknowledgements:

This work is Supported by the National Natural Science Foundation of China (Nos. 10875133, 10821063, 11035006), the Chinese Academy of Sciences Knowledge Innovation Project (Nos. KJCX2-EW-N01), the Ministry of Science and Technology of China

(2009CB825200), and the U.S. Department of Energy, Office of Nuclear Physics Division, under Contract No. DE-AC02-06CH11357.

[1] Particle Data Group, C. Amsler *et al.*, Phys. Lett. **B 667**, 1 (2008).

[2] S. Capstick and W. Roberts, Prog. Part. Nucl. Phys. **45**, S241 (2000).

[3] B. C. Liu, B. S. Zou, Phys. Rev. Lett. **96**, 042002 (2006); ibid, **98**, 039102 (2007).

[4] N. Kaiser, P. B. Siegel and W. Weise, Phys. Lett. B **362**, 23 (1995).

[5] E. Oset and A. Ramos, Nucl. Phys. A **635**, 99 (1998).

[6] J. A. Oller, E. Oset and A. Ramos, Prog. Part. Nucl. Phys. **45**, 157 (2000).

[7] J. A. Oller and U. G. Meissner, Phys. Lett. B **500**, 263 (2001).

[8] T. Inoue, E. Oset and M. J. Vicente Vacas, Phys. Rev. C **65**, 035204 (2002)

[9] C. Garcia-Recio, M. F. M. Lutz and J. Nieves, Phys. Lett. B **582**, 49 (2004).

[10] T. Hyodo, S. I. Nam, D. Jido and A. Hosaka, Phys. Rev. C **68**, 018201 (2003)

[11] C. Helminen and D. O. Riska, Nucl. Phys. A **699**, 624 (2002).

[12] B. S. Zou, Nucl. Phys. A **835**, 199 (2010).

[13] S. J. Brodsky, P. Hoyer, C. Peterson and N. Sakat, Phys. Lett. **B 93**, 451 (1980).

[14] J. -J. Wu, R. Molina, E. Oset, B. S. Zou, Phys. Rev. Lett. **105**, 232001 (2010). Phys. Rev. **C84**, 015202 (2011).

[15] W. L. Wang, F. Huang, Z. Y. Zhang, B. S. Zou, Phys. Rev. **C84**, 015203 (2011).

[16] Z. -C. Yang, Zhifeng Sun, J. He, X. Liu, S. -L. Zhu, [arXiv:1105.2901 [hep-ph]].

[17] A.D. Lahiff and I.R. Afnan, PHys. Rev. C**66**,044001 (2002)

[18] T. Sato and T.-S. H. Lee, Phys. Rev. C**54**, 2660 (1996).

[19] As reviewed by A. Klein and T.-S. H. Lee, Phys. Rev. D**10**, 4308 (1974)

[20] B.C. Pearce and B.K. Jennings, Nucl. Phys. **528**. 655 (1991)

[21] T. Hung, S.N. Yang, and T.-S. H. Lee, Phys. Rev. C**64**, 034309 (2001)

[22] R. Macheleidt, Adv. Nucl. Phys. **19**, (1979)

[23] A. Matsuyama, T. Sato and T. S. Lee, Phys. Rept. **439**, 193 (2007) [arXiv:nucl-th/0608051].

[24] B. Julia-Diaz, T. -S. H. Lee, A. Matsuyama, T. Sato, Phys. Rev. **C76**, 065201 (2007). [arXiv:0704.1615 [nucl-th]].

[25] N. Suzuki, T. Sato, and T.-S. H. Lee, Phys. Rev. C**79**. 025205 (2009)

[26] J. J. Wu, L. Zhao, and B. S. Zou, arXiv:1011.5743 [hep-ph], Phys. Lett. B (2012), doi:10.1016/j.physletb.2012.01.068.